ONCOIMMUNOLOGY
2023, VOL. 12, NO. 1, 2164476
https://doi.org/10.1080/2162402X.2022.2164476

Taylor & Francis
Taylor & Francis Group

ORIGINAL RESEARCH

OPEN ACCESS Check for updates

Tertiary lymphoid structures in desmoplastic melanoma have increased lymphocyte density, lymphocyte proliferation, and immune cross talk with tumor when compared to non-desmoplastic melanomas

Nicole L. Edmonds[a,b], Sarah E Gradecki[c], Priya Katyal[b,d], Kevin T Lynch[b], Anne M Stowman[e], Alejandro A Gru[c], Victor H Engelhard[f,g], Craig L Slingluff Jr.[b,g], and Ileana S. Mauldin[b,g]

[a]School of Medicine, University of Virginia, Charlottesville, VA, USA; [b]Department of Surgery, University of Virginia Health System, Charlottesville, VA, USA; [c]Department of Pathology, University of Virginia Health System, Charlottesville, VA, USA; [d]College of Arts and Sciences, University of Virginia, Charlottesville, VA, USA; [e]Department of Pathology, University of Vermont Medical Center, Burlington, VA, USA; [f]Department of Microbiology, Immunology, and Cancer Biology, University of Virginia School of Medicine, Charlottesville, VA, USA; [g]Beirne B. Carter Center for Immunology Research, University of Virginia School of Medicine, Charlottesville, VA, USA

ABSTRACT

Tertiary lymphoid structures (TLS) are ectopic lymphoid structures that can arise in human cancers and are associated with improved overall survival (OS) and response to immune checkpoint blockade (ICB) in several cancers, including non-desmoplastic metastatic melanoma (NDMM). Desmoplastic melanoma (DM) has one of the highest response rates to ICB, and we previously identified that primary DM (PDM) contains TLS. Despite the association of TLS with survival and ICB response, it is unknown whether TLS or associated markers of immune activity can differ between PDM and NDMM. We hypothesized that PDM would contain higher frequencies of TLS than NDMM, that T and B-cell densities and proliferation would be greater in TLS of PDM than TLS of NDMM, and that proliferation rates of T and B-cells in PDM TLS would be concordant with those of intratumoral lymphocytes. We found that four features of TLS in PDM distinguish them from TLS in NDMM. TLS were peritumoral in NDMM but intratumoral in PDM. $CD8^+$ T-cell and $CD20^+$ B-cell densities and proliferative fractions were higher in PDM TLS than NDMM TLS. Additionally, the proliferative fractions of T- and B-cells were concordant between the TLS and tumor site in PDM and discordant in NDMM. Collectively, these data suggest that TLS and associated immune markers can differ across melanoma subsets and suggest that PDM TLS may be more immunologically active and have enhanced immune cell trafficking between tumor and TLS compared to NDMM.

ARTICLE HISTORY
Received 12 September 2022
Revised 19 December 2022
Accepted December 26, 2022

KEYWORDS
Immunology; tumor infiltrating lymphocytes; multiplex immunofluorescence histology; tertiary lymphoid structures; melanoma; desmoplastic melanoma

Introduction

Desmoplastic melanoma (DM) is an uncommon variant of melanoma which has a higher tumor mutation burden than non-desmoplastic cutaneous melanomas and one of the highest response rates to single-agent PD-1 blockade therapy in any cancer, with objective tumor responses rates (ORR) in 70% of the patients.[1,2] Primary DM (PDM) has three key histologic features: (i) a lentiginous melanocytic proliferation along the dermo-epidermal junction, (ii) a dermal spindle cell population within the desmoplastic stroma, and (iii) intratumoral lymphoid aggregates.[3] In our previous work, we found that some of these lymphoid aggregates in PDM comprise tertiary lymphoid structures (TLS).[3]

TLS are ectopic lymphoid structures that are induced by sustained antigenic stimulation in inflamed, infected, or neoplastic tissues.[4] Histologically, TLS are most commonly defined by the presence of discrete, organized T and B-cell compartments with at least one of the following: $PNAd^+$ high endothelial venules (HEV), mature dendritic cells (DC) in the T-cell areas, or a gene signature that includes CCL19, CCL21, CXCL12, and CXCL13.[5–8] TLS are believed to aid in generating antigen-driven immune responses outside of the spleen, lymph nodes, and other secondary lymphoid organs.[9]

In cancers, including non-desmoplastic melanomas, TLS have been associated with higher rates of disease-free survival and clinical response to immunotherapy with PD-1 antibody therapy.[4,9,10] Similarly, our prior studies found that TLS in cutaneous NDMM were independently associated with improved overall patient survival, thus highlighting the importance of TLS as an independent prognostic factor for NDMM.[11] It is believed that TLS improve cancer prognosis by serving as sites for expansion of tumor-reactive T-cells and B-cells that can then be home to adjacent tumors and continue to proliferate there.[9,12] Thus, finding TLS in PDM raises the possibility that they may support anti-tumor immunity to PDM tumors.

The high rates of clinical response of DM to immune therapy raise the possibility that TLS in DM may support stronger adaptive anti-tumor immunity. Interestingly, we have found that TLS in PDM were exclusively located intratumorally,[3] leading us to anticipate that T- and B-cells expanded in those TLS may not encounter the same barriers to infiltrating the tumor compartment as in NDMM. In the present work, we

CONTACT Ileana S. Mauldin is3v@virginia.edu University of Virginia, 345 Crispell Drive, PO Box 801329 A 22908 Charlottesville, VA, USA
Supplemental data for this article can be accessed online at https://doi.org/10.1080/2162402X.2022.2164476

hypothesized that TLS would be more prevalent and numerous in PDM than NDMM. Furthermore, we hypothesized that the TLS from PDM would contain increased densities of lymphocytes and higher proportions of proliferating ($Ki67^+$) $CD20^+$ B-cells and $CD8^+$ T-cells relative to NDMM. Additionally, we hypothesized that lymphocytic proliferation rates within TLS from PDM would correlate with lymphocytic proliferation rates within tumor.

Methods

Patient selection and TLS identification

PDM:

With institutional IRB approval (IRB #19694), 11 cases of "pure" primary desmoplastic melanoma located on the skin or subcutaneous tissues that met inclusion criteria in our prior work[3] were included in this study. Eight of these samples were determined, in our prior work to have classical TLS, defined by organized T-cell and B-cell regions in addition to $PNAd^+$ vasculature.[3]

NDMM:

With institutional IRB approval (IRB-HSR #10803), 64 checkpoint-therapy naïve patients with stage IIIB–IV melanoma metastatic to the skin or subcutaneous tissues that met inclusion criteria were evaluated in our prior work,[11] and 30 were found to have classical TLS.

Clinical data collection

Clinical data for PDM and NDMM patients were collected from the electronic medical record (EPIC) and melanoma patient database (IRB #19694 and #10803) and published previously.[3,11] Staging for PDM samples was performed for the present work using the American Joint Committee on Cancer (AJCC) melanoma staging system (8^{th} version).[13] Staging for NDMM samples was previously published using these same AJCC guidelines. Clinical data were then compared between PDM and NDMM patients in the current study using the Chi-Square test for categorical data and Mann Whitney test for continuous data. Those performing multiplex immunohistochemistry and image analysis were blinded to patient HIPAA identifiers and clinical data.

Multiplex immunofluorescence histology and imaging

Five μm thick sections were cut from FFPE tumor specimens. Multiplex immunofluorescence histology (mIFH) was performed according to the manufacturer's protocol using the OPAL Multiplex Manual IHC kit, and antigen retrieval (AR) buffers AR6 and AR9 (Akoya Biosciences, Marlborough, Massachusetts, USA). Staining sequence, antibodies, and AR buffers were as follows for the TLS identification panel:

AR9, CD8 (1:500, clone C8/144B Agilent Technologies, Santa Clara, California, USA) Opal540; AR6, CD20 (1:1000, clone L26, Agilent Technologies) Opal520; AR6, PNAd (1:1000 clone MECA-79, BioLegend, San Diego, California, USA) Opal620; AR6, Ki67 (1:20, SP6, Abcam, Cambridge, Massachusetts, USA) Opal690; and AR6, spectral DAPI (Akoya Biosciences, Marlborough, Massachusetts, USA).

Following staining, slides were mounted using prolonged diamond antifade (Life Technologies, Carlsbad, California, USA) and scanned using the PerkinElmer Vectra V.3.0 system and Vectra software (Akoya Biosciences, Marlborough, Massachusetts, USA). Regions of interest (ROI) were selected in Phenochart software (Akoya Biosciences, Marlborough, Massachusetts, USA) that evaluated the whole tumor specimen for PDM and NDMM. Additionally, in NDMM specimens an additional scan and ROI selection was performed on each B-cell cluster regardless of location intratumorally and peritumorally. 20x magnification images were acquired of each ROI with the Vectra V.3.0 system, and images were then spectrally unmixed using single stain positive control images in InForm software (Akoya Biosciences, Marlborough, Massachusetts, USA).

Image analysis

B-cell clusters that were identified as TLS were further subdivided from the surrounding tissue using HALO Software (Indica Labs, Albuquerque, New Mexico, USA) for analyses of intra-TLS lymphocytes in this study. Specifically, an individual box was drawn around the TLS in HALO for both PDM and NDMM specimens. B- and T-cell areas were bounded, using $PNAd^+$ vasculature to define the border periphery. This enabled analyses of intra-TLS lymphocytes from other intratumoral lymphocytes in PDM, and enabled a uniform analysis of TLS T-cell regions in both PDM and NDMM. Immune cells were quantified using HALO software (Indica Labs, Albuquerque, New Mexico, USA). Lymphocyte density was quantified as density of cells expressing a given marker (cells/mm^2) within the ROI. Fractions of lymphocytes expressing a given activation marker were calculated by normalizing the density of cells expressing the lymphocyte marker and the activation marker by the density of cells expressing the lymphocyte marker (Example: Fraction of $Ki67^+CD8^+$ T-cells = $CD8^+Ki67^+/CD8^+$). Fractions where the denominator was zero were treated as zeros. TLS areas reported in **Supplemental Table S1** were quantified using HALO software. Measurements of the total specimen areas reported in **Supplemental Table S1** were obtained on H&E stained specimens and analyzed using ImageJ software.[14]

Statistical analysis

The Chi-Squared test was used to compare categorical variables between NDMM and PDM including the total number of tumor samples with TLS, the percentage of female patients, and the percentage of patients at each stage of disease. The Mann–Whitney U-test was performed to compare continuous variables between PDM and NDMM, including age as well as the density and proliferation index of immune cells. The Wilcoxon signed-rank test was performed to compare the density and proliferation index of immune cells between TLS and tumor of the same patient specimen. Spearman's rank correlation coefficient was used to compare lymphocyte proliferation index intratumorally and peritumorally as well as to compare B-cell proliferation index to T-cell proliferation

index. P values were considered significant when < 0.05. All statistical analyses were performed using R software V.3.5.3 and Microsoft Excel.

Results

Patient demographics

The median age of the 30 patients with NDMM containing TLS was 56. Nineteen patients (63%) were female, 17 (57%) had AJCC stage IIIB disease, and 13 (43%) had stage IV disease. Among the patients with PDM containing TLS, the median age was 67. Two patients (25%) were female, one (12.5%) had stage 1 disease, and seven (88%) had stage 2 disease. The median PDM tumor thickness was 4.7 mm with a range of 1.8 mm-20.8 mm. As expected, the patients with PDM had a less advanced stage than the patients with NDMM. Age and gender were not significantly different between groups. Clinical data, survival status, and information on TLS are provided for each of the evaluated PDM patients and NDMM patients in **Supplemental Tables S2 and S3**, respectively. The sample size for the PDM patients is not large enough to make formal analyses about outcome, but six of the eight patients with TLS^+ PDM (75%) are currently alive with a median follow-up of 75 months, while only one of the three TLS^{neg} PDM (33%) patients are currently alive with a median follow-up of 37 months. For NDMM patients, analyses of associations between TLS and clinical outcome have already been reported.[11]

Frequency and size of TLS in tumor samples

In prior work, we reported on the proportions of tumors that have TLS among the NDMM samples (47%, 30/64) and PDM samples (73%, 8/11).[3,11] However, we had not previously compared them or tested for differences in those proportions. The percentage of patients whose tumors contained TLS trended higher for PDM (73%) than for cutaneous NDMM (47%); however, this difference was not significant with these sample sizes (p = .116, chi-square).

Among the 30 NDMM samples with TLS, the median number of TLS per specimen was 4. Among the 8 PDM samples with TLS, the median number of TLS per specimen was 1.5 (p = .019). The total specimen area was not significantly different between groups (p = .56). Nevertheless, the number of TLS per tumor was also assessed after normalizing for the tumor cross-sectional area. The median numbers of TLS per cm^2 specimen area were 1.99 for NDMM and 0.92 for PDM (p = .019). Thus, among melanomas for which TLS were identified, they were less numerous in PDM than in NDMM. The size of the TLS in PDM and NDMM were also compared. The median TLS area (mm^2) was 0.10 in PDM and 0.52 in NDMM (p = .02). Thus, TLS were smaller in size in PDM. The data for the TLS areas (mm^2), biopsy specimen areas (cm^2), numbers of TLS per biopsy, and numbers of TLS per biopsy normalized for the specimen cross-sectional area are provided in **Supplemental Table S1**.

Comparison of TLS location in tumor samples

In our prior work, we described TLS as being more commonly intratumoral in PDM and peritumoral in NDMM but did not evaluate the frequency of TLS location. In this assessment, we have noted that in the 8 PDM with TLS, all TLS in all eight samples (100%) were intratumoral, and none were peritumoral. On the other hand, for all 30 of the NDMM with TLS, all TLS in all 30 samples (100%) were peritumoral, and none were intratumoral. This difference in location is significant (p < .001, chi-square). Examples of the TLS locations for PDM and NDMM are shown by H&E staining Figures 1A and 1B, respectively, to illustrate the location of the TLS relative to tumor areas. TLS were identified by mIFH, shown in Figure 1(C-H) for a TLS containing PDM specimen, and Figure 1(I-N) for an NDMM TLS-containing specimen. .

Comparison of lymphocyte density in PDM And NDMM TLS

The numbers of $CD8^+$ T-cells and $CD20^+$ B-cells per TLS were enumerated using mIFH with $PNAd^+$ cells as the boundary of T-cell regions. The median number of $CD8^+$ T-cells per TLS were 91 and 218 in PDM and NDMM respectively (p = .30, data not shown). The median number of $CD20^+$ B-cells per TLS were 416 and 394 in PDM and NDMM respectively (p = .69, data not shown). The total TLS area was larger in NDMM, thus we also evaluated the density of T and B cells per mm^2. Median numbers of $CD8^+$ T-cells in TLS per mm^2 were 870 and 281 for PDM and NDMM, respectively (p = .0007, (Figure 2A)). Similarly, the median densities of $CD20^+$ B-cells in TLS per mm^2 were 2,508 and 578 for PDM and NDMM, respectively (p < .0001, (Figure 2B)). Thus, PDM TLS contained higher densities of B and T-cells than TLS in NDMM.

Comparisons of lymphocyte proliferative activity in TLS and tumor of both PDM and NDMM

Antigen-driven adaptive immune responses induce proliferation of T and B-cells, which can be identified by nuclear expression of Ki67. The numbers of proliferating $CD8^+$ T-cells and $CD20^+$ B-cells per TLS were compared between PDM and NDMM. The median number of proliferating $CD8^+$ T cells per TLS were 43 and 16 in PDM and NDMM respectively (p = .02, data not shown). The median number of proliferating $CD20^+$ B-cells per TLS were 157 and 13 in PDM and NDMM respectively (p = .001, data not shown). We also considered the density of proliferating T and B cells per mm^2. TLS within PDM had more $CD8^+Ki67^+$ T-cells per mm^2 (median 389 cells/mm^2) than TLS of NDMM (18 cells/mm^2; p = .0006, (Figure 3A)). Similarly, PDM TLS had more $CD20^+Ki67^+$ B-cells per mm^2 (median 1,182 cells/mm^2) than NDMM-TLS (13 cells/mm^2, p = .00002, (Figure 3B)). The densities of proliferating B and T-cells were significantly greater in TLS compared to tumor for both PDM and NDMM, except for proliferating $CD8^+$ T-cells in NDMM TLS, which were significantly lower than NDMM tumor (median 18 cells/mm^2 NDMM TLS, 42 cells/mm^2 NDMM tumor, p = .0015, Wilcoxon signed-rank test, Figure 3A).

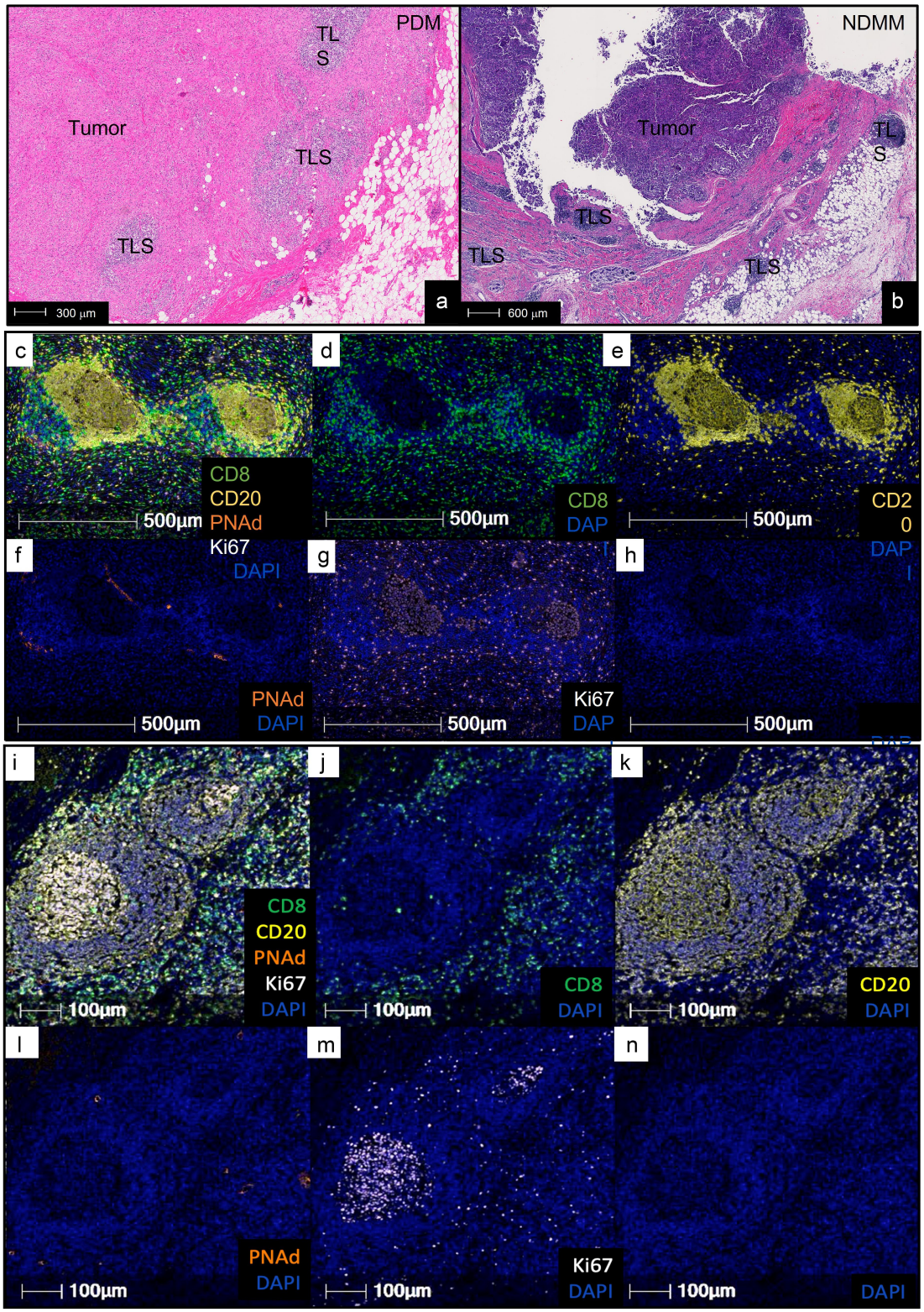

Figure 1. Representative images of TLS in PDM and NDMM. Images from hematoxylin and eosin (H&E)-stained tumor sections show the location of TLS relative to tumor in PDM (A) and in NDMM (B). Multiplex and single marker images of TLS in PDM (C-H) and NDMM (I-**N)** show the markers evaluated in this study. Images are of the 5-color multiplex stain (C, I) as well as single marker stains depicting CD8 (D, J), CD20 (E, K), PNAd (F,L), and Ki67 (G,M) in combination with DAPI shown in blue and alone in (H, N). Marker colors and image magnifications are indicated.

As stated above, the density of T and B-cells is higher in PDM than NDMM, thus the significance of the increased density of proliferating lymphocytes may simply reflect the greater density of lymphocytes in PDM. Thus, we also determined the fractions of lymphocytes proliferating ($Ki67^+$) within the TLS and associated tumor regions. The fractions of proliferating ($Ki67^+$) $CD8^+$ T-cells were higher in TLS of PDM than in TLS of NDMM (medians 47% and 7%, respectively,

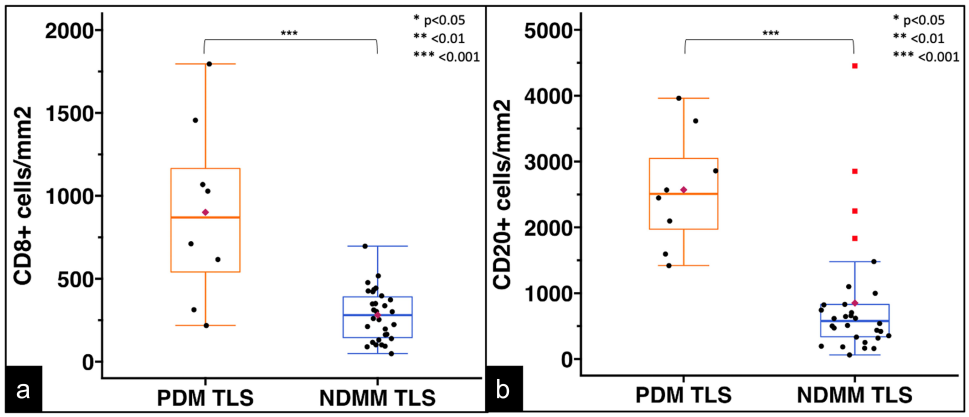

Figure 2. T- and B-cell densities in TLS from PDM and NDMM. Box plots of $CD8^+$ T-cell (A) and $CD20^+$ B-cell (B) densities within TLS from PDM and NDMM are plotted. The central box represents values from the lower to upper quartile, 25th to 75th percentile. The middle bar identifies the median, the maroon diamond depicts the mean, whiskers show minimum and maximum, and outliers are shown as red squares. Statistical comparisons were made by Mann-Whitney U test; ***p < .001.

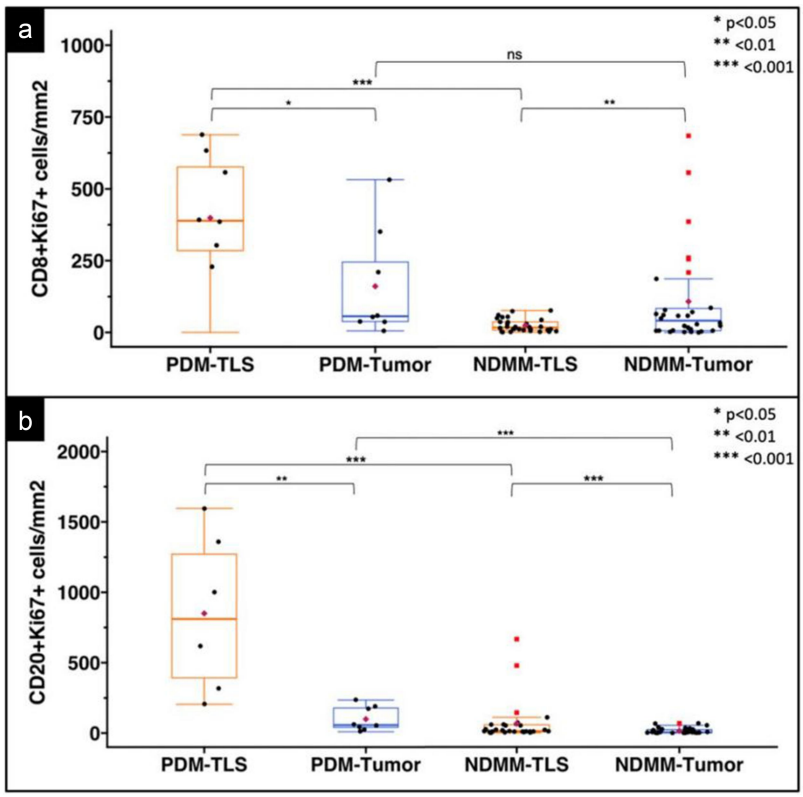

Figure 3. Densities of proliferating B- and T-cells in TLS and tumor of PDM and NDMM. Box plots of $CD8^+Ki67^+$ T-cells (A) and $CD20^+Ki67^+$ B-cells (B) densities at the TLS and tumor site of PDM and NDMM. The central box represents values from the lower to upper quartile, 25th to 75th percentile. The middle bar identifies the median, the maroon diamond depicts the mean, whiskers show minimum and maximum, and outliers are shown as red squares. Statistical comparisons were made by the Mann-Whitney U test when comparing cell densities across PDM and NDMM specimens and by the Wilcoxon signed-rank tests when comparing cell densities at the TLS and tumor site within the same biopsy specimen; *p < .05; **p < .01; ***p < .001.

p = .0014, (Figure 4A)). Similarly, the fractions of proliferating ($Ki67^+$) $CD20^+$ B-cells within the B-cell compartment were higher in TLS of PDM than in TLS of NDMM (medians 53% and 4%, respectively, p < .0001, (Figure 4B)).

Interestingly, lymphocyte proliferative fractions were high within TLS of most PDM as well as within adjacent tumor areas (excluding TLS areas), and those proportions were similar between TLS and tumor. The median proliferative fractions of $CD8^+$ T-cells in PDM were 47% and 41% for TLS and tumor, respectively (p = .96, Wilcoxon signed-rank test, Figure 4A). Similarly, proliferative fractions of $CD20^+$ B-cells were 53% and 48% for TLS and tumor, respectively (p = .96, Figure 4B). In contrast, for NDMM, the proliferative fractions were much lower in TLS than in tumor: median proliferative fractions for $CD8^+$ T-cells were 41% and 7% for tumor and TLS, respectively (p < .00001, (Figure 4A)) and for $CD20^+$ B-cells, median proliferative fractions were 23% and 4% for tumor and TLS, respectively (p < .00001, (Figure 4B)).

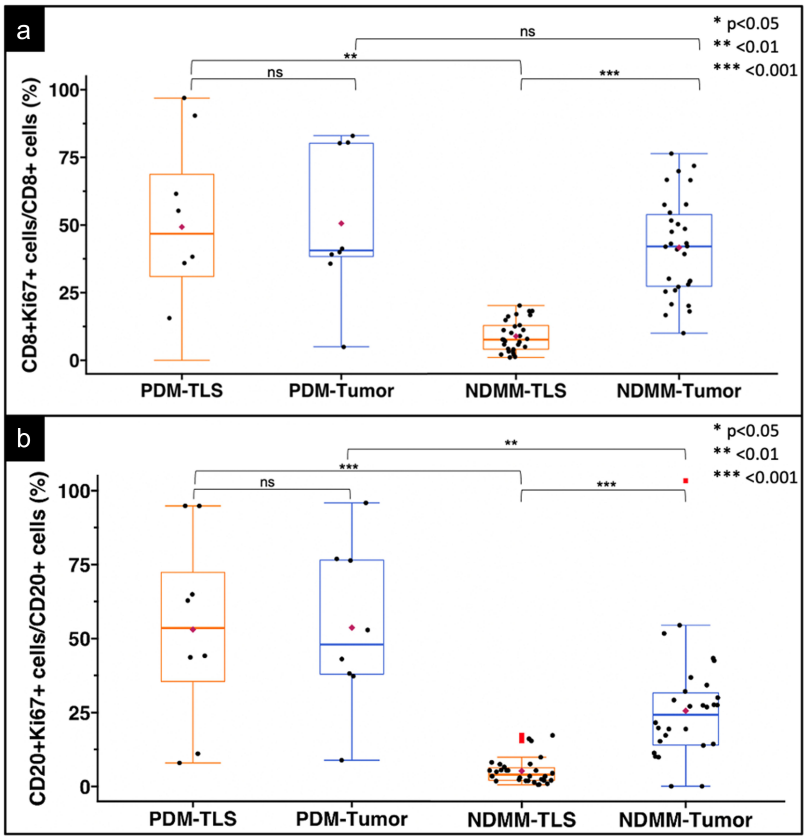

Figure 4. Proportions of proliferating T- and B-cells in the TLS and tumor site of PDM and NDMM. Box plots of the proportions of proliferating $CD8^+Ki67^+$ T-cells (A) or $CD20^+Ki67^+$ B-cells (B) at the TLS and tumor site in PDM and NDMM. The central box represents values from the lower to upper quartile, 25th to 75th percentile. The middle bar identifies the median, the maroon diamond depicts the mean, whiskers show minimum and maximum, and outliers are shown as red squares. Statistical comparisons were made by the Mann-Whitney U test when comparing cell proportions across PDM and NDMM specimens and by the Wilcoxon signed-rank tests when comparing cell proportions at the TLS and tumor site within the same biopsy specimen; **p < .01; ***p < .001.

Comparisons of lymphocyte density and proliferative activity in TLS and tumor of PDM by stage and BRAF mutational status

The impact of tumor stage or BRAF mutational status on lymphocyte density in melanoma associated TLS is unknown. In our evaluated TLS containing NDMM subset, 17 specimens were stage 3 and 13 were stage 4, additionally 12 specimens were BRAF wild-type, 16 contained the BRAF V600E mutation and 2 specimens were unclassified (Supplemental Table S1). In the TLS positive PDM cohort, 7 PDM were stage 2 and 1 specimen was stage 1, of these 1 specimen was BRAF wild-type; and the other seven were unknown (Supplemental Table S1). However, BRAF mutations are not commonly found in desmoplastic melanomas[15–17] and BRAF mutational status is not typically evaluated in specimens that are of a lower stage. Thus, the densities of $CD8^+$ T-cells and $CD20^+$ B-cells, numbers of proliferating lymphocytes and lymphocyte proliferative fractions, and per TLS and tumor were compared in NDMM specimens by stage (3 vs. 4) and BRAF mutational status (wild-type vs. V600E). No significant differences were found in the densities of $CD8^+$ T-cells and $CD20^+$ B-cells, numbers of proliferating lymphocytes, or lymphocyte proliferative fractions between stage 2 and stage 4 NDMM specimens in the TLS or tumor site (Supplemental Figure S1). Additionally, no significant differences were found in the densities of $CD8^+$ T-cells and $CD20^+$ B-cells, numbers of proliferating lymphocytes, or lymphocyte proliferative fractions between BRAF wild-type or BRAFV600E containing NDMM in TLS or tumor site (Supplemental Figure S2).

Correlations between proliferating $CD8^+$ T and $CD20^+$ B-cells

These findings that T-cell and B-cell proliferative fractions are similar between the TLS and tumor compartments of PDM raise questions about whether T- and B-cell proliferation are similar within the same compartment. Within TLS, it may be reasonable to expect that the organized T- and B-cell areas function in an integrated way so that adaptive T-cell responses in the T-cell compartment may be associated with proliferative responses in the B-cell compartment in the same TLS. Thus, we also assessed whether the proliferative ($Ki67^+$) fraction of B and T-cells were correlated with each other within TLS, as well as whether they were correlated with each other within tumor compartments. In PDM with TLS, significant correlations were noted between the proliferative fractions of $CD8^+$ T-cells and $CD20^+$ B-cells within the TLS ($R = 0.95$, $p = .001$, Figure 5A). The associations were significant but slightly weaker within the tumor areas ($R = 0.76$, $p = .037$, Figure 5B). For NDMM, significant correlations were also noted between proliferative fractions of $CD8^+$ T-cells and B-cells within the TLS ($R = 0.59$, $p < .001$, Figure 5C) as well

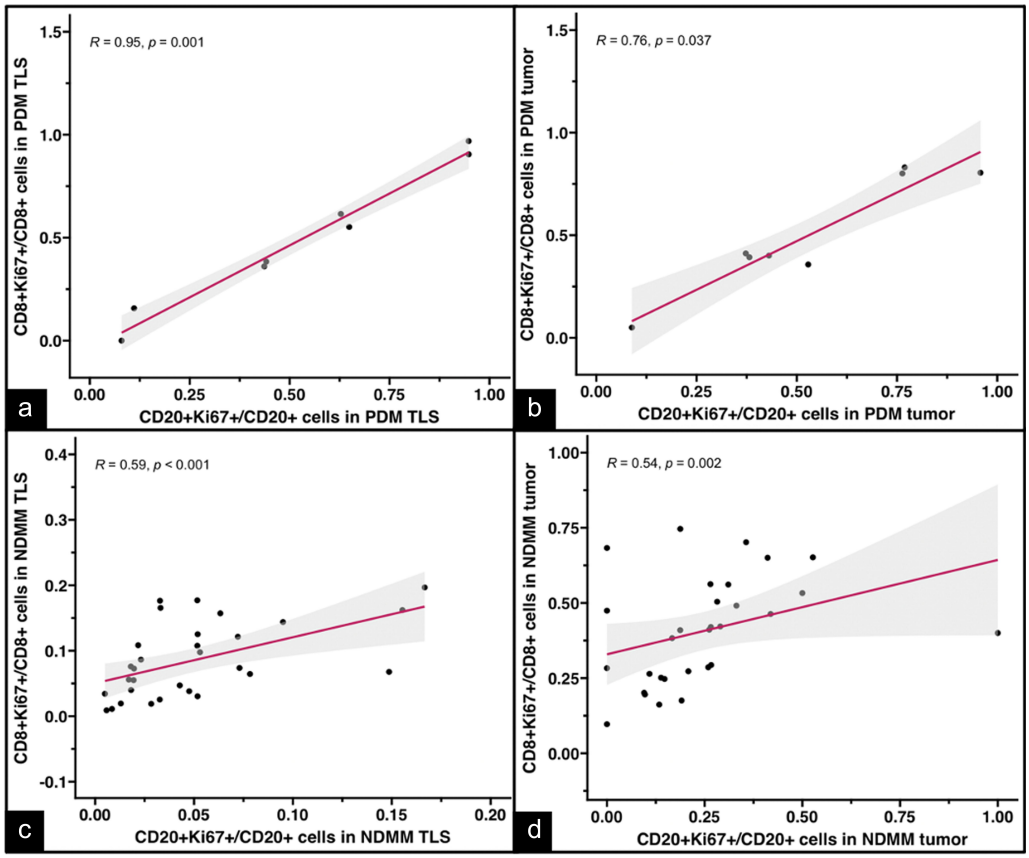

Figure 5. Correlation graphs comparing the fraction of proliferating T and B-cells within the TLS compartment and within the tumor compartment of PDM and NDMM. Correlation graphs comparing the relationship between the fraction of proliferating B and T-cells within the TLS for PDM (A) and NDMM (C); and the relationship between the fractions of intratumoral, proliferating B and T-cells in PDM (B) and NDMM (D). Correlation coefficient (R) and p values calculated by Spearman's rank correlation test.

as within the tumor (R = 0.54, p = .002, Figure 5D), though those correlation coefficients for NDMM were lower than for PDM.

Correlations between proliferative fractions of lymphocytes in tumor and TLS

The findings that B- and T-cell proliferation are correlated within the TLS and tumor compartments suggest that these cells are proliferating in concert within the same compartment. We also assessed whether the fractions of proliferating ($Ki67^+$) T and B-cells correlated between TLS and tumor compartments. In PDM, significant correlations were noted between the fractions of proliferating ($Ki67^+$) $CD8^+$ T-cells within TLS and the tumor (R = 0.76, p = .037, Figure 6A) as well as between the fractions of proliferating ($Ki67^+$) $CD20^+$ B-cells within TLS and the tumor (R = 0.95, p = .001, Figure 6B). In contrast, for NDMM, significant correlations were not found between the fractions of proliferating ($Ki67^+$) $CD8^+$ T-cells within TLS and the tumor (R = 0.20, p = .297, Figure 6C). We had previously reported that the fractions of proliferating ($Ki67^+$) $CD20^+$ B-cells within TLS and the tumor were not concordant in NDMM.[13] For the present work, we used new boundary definitions for TLS (see Methods), with similar findings of poor concordance between the proliferative fractions of B-cells of TLS and tumor for NDMM (R = 0.13, p = .478, Figure 6D).

Discussion

This study follows on two prior studies, one being the first to identify the immune cell aggregates in desmoplastic melanoma to be TLS[3] and the other having identified features of TLS associated with survival for cutaneous NDMM.[11] In the present report, we have evaluated these further and compared the TLS of PDM to the TLS of NDMM, both in cutaneous sites. We have identified four key features of TLS in PDM that distinguish them from TLS in NDMM: (1) intratumoral location, (2) increased densities of T- and B-cells, (3) higher proliferative fractions of $CD20^+$ and $CD8^+$ cells, (4) concordance of lymphocyte proliferation rates between TLS and tumor areas.

We had hypothesized that PDM samples would contain higher frequencies and numbers of TLS. While the proportion of PDM samples containing TLS trended higher than NDMM, this did not reach statistical significance. Furthermore, the number of TLS per tumor was lower in PDM with TLS than in NDMM with TLS, raising the possibility that the immunologic activity within the TLS or immunologic "quality" of TLS may be more important than the quantity of TLS. We did find that PDM TLS had increased T and B-cell densities and proliferative fractions relative to NDMM TLS. Thus, these data suggest that adaptive immune responses may be enhanced in PDM TLS. Such differences may be due to greater antigen exposure, less immune cell inhibition, or enhanced dendritic

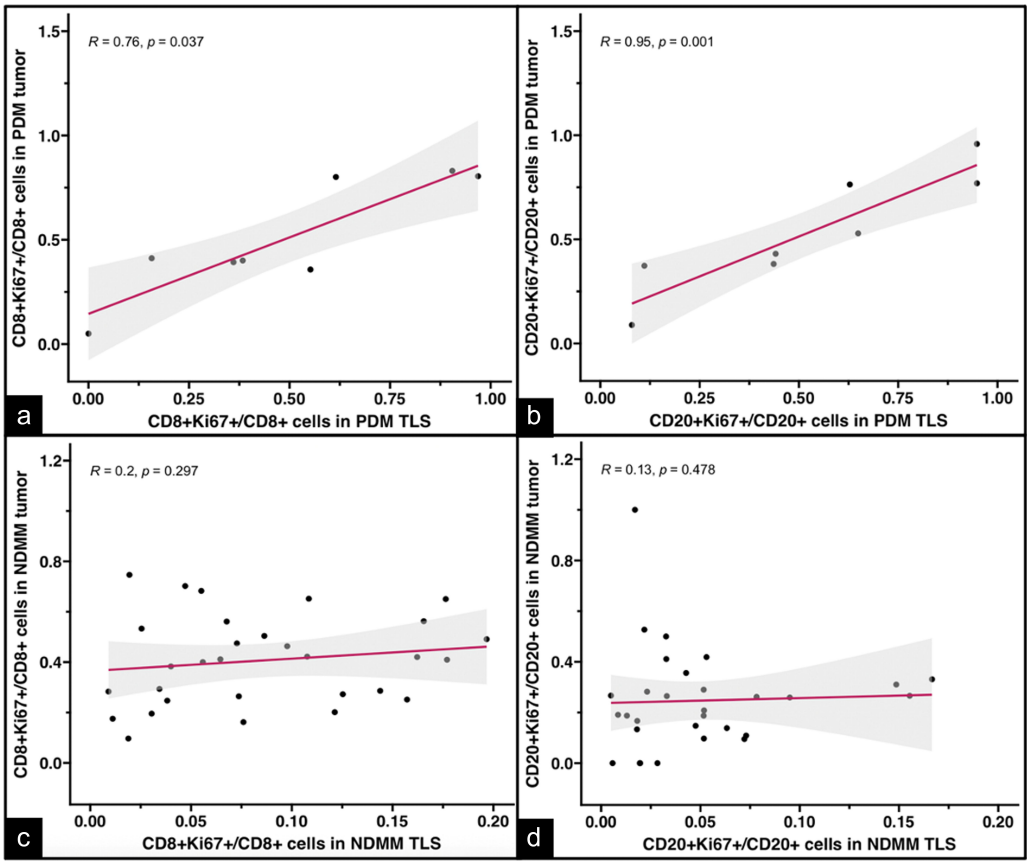

Figure 6. Correlation graphs comparing the fraction of proliferating T- and B-cells at the TLS site and matched tumor site, in PDM and NDMM. Correlation graphs showing the relationship between the fractions of proliferating $CD8^{+}Ki67^{+}$ T-cells at the TLS site to those in the matched tumor in PDM (A) and NDMM (C); and the proportions of proliferating $CD20^{+}Ki67^{+}$ B-cells at the TLS site to those in the matched tumor in PDM (B) and NDMM (D). Correlation coefficient (R) and p values calculated by Spearman's rank correlation test.

cell maturation. Thus, future studies are warranted to address these mechanistic questions.

We also found that the fractions of proliferating and T- and B-cells were correlated between the TLS and tumor compartments of PDM. Conversely, in NDMM, the intra-tumoral and intra-TLS lymphocyte proliferation rates were not correlated. The concordance of proliferative fractions in TLS and tumor of PDM suggests crosstalk or active trafficking of T-cells between tumor and TLS areas. These findings could be explained by PDM's unique intratumoral TLS location compared to the extratumoral location of NDMM TLS.[3,11] In pancreatic cancer, extratumoral TLS density was not a prognostic marker, but intratumoral TLS functioned as an independent favorable prognosticator.[18] Therefore, the intratumoral TLS in DM could have important prognostic implications, and future studies that investigate T cell trafficking in these specimens are needed.

There were limitations to this study. One is the limited sample size of PDM, which reflects the low incidence rate of desmoplastic melanoma in the population (two per million).[19] Another potential limitation of our study is that we compared primary cutaneous desmoplastic melanomas to cutaneous metastatic melanoma. It may seem to be more logical to compare PDM to primary non-desmoplastic melanomas or metastatic DM to metastatic non-desmoplastic melanomas. However, prior studies have reported that classical TLS, as we have defined in this study, are rarely present in primary non-desmoplastic melanomas.[20,21] Thus, we focused our analyses on NDMM, where classical TLS have been reported in up to 55% of the cases.[20,21] Additionally, DM metastasis has been reported to occur primarily in mixed subtypes of DM, which contain portions of non-desmoplastic melanoma and thereby may lack the unique dysplasia and stromal features of DM throughout the tumor.[22] Thus, we opted to analyze pure PDM samples with unique desmoplastic stroma present and NDMM samples with classical TLS. Future studies evaluating the prevalence of TLS in primary desmoplastic melanomas metastases and non-desmoplastic melanoma metastases are underway and evaluations of lymphocytic densities and activity in these TLS are warranted.

This current study is not powered to assess associations between TLS status and survival in patients with PDM. In our prior work with patients with non-desmoplastic cutaneous melanoma metastases, we found that the presence of TLS was associated with improved OS in patients treated with surgery prior to the checkpoint blockade therapy era.[11] Others have reported that TLS are associated with response to checkpoint blockade therapy in non-DM patients.[10,23,24] Thus, it is reasonable to hypothesize that desmoplastic melanomas may have higher response rates to checkpoint blockade therapy when TLS are found. A larger study is warranted and planned, to test whether PDM with TLS have better clinical outcomes than

those without TLS, and whether patients with metastatic DM are more likely to respond to checkpoint blockade therapy when TLS are found in the metastatic lesions. Recent data from a small study of 27 patients demonstrated a 56% pathological complete response rate when pembrolizumab was employed in the neoadjuvant setting for patients with resectable DM. These findings raise the question of whether TLS may predict response to short-term PD-1 blockade, and whether surgical resection may be reduced or avoided in patients that respond to checkpoint blockade therapy. Thus, future studies evaluating the association between the presence of TLS and OS in patients with PDM treated with checkpoint blockade therapy are warranted.

In conclusion, this is the first study, to our knowledge, that has compared markers of immune activity between desmoplastic and non-desmoplastic subtypes of melanoma. We have identified features of TLS in PDM that distinguish them from TLS in NDMM and which suggest increased immunologic activity and lymphocyte trafficking between TLS and tumor in PDM. These unique immunologic features may contribute to high response rates of DM to ICB and warrant further study to better characterize the immunologic activity in a larger sample size. The present study has focused on proliferation as a marker of immunologic activity, but future studies could evaluate markers of TLS maturation, B-cell activity, and T-cell activity to evaluate whether effector B and T cells are enhanced in DM related to non-DM. T-cell receptor (TCR) sequencing studies could also aid in the assessment of T cell trafficking between tumor and TLS sites.

Acknowledgments

We thank the Molecular and Immunologic Translational Studies Core and the Biorepository and Tissue Research Facility for help with these studies. Additionally, we thank Samuel Young and Adela Mahmutovic for their assistance with staining samples and Marieke Jones for assistance with statistical analyses.

Disclosure statement

Dr. Slingluff has the following disclosures, none of which conflict with the present manuscript: Research support to the University of Virginia from Celldex (funding, drug), Glaxo-Smith Kline (funding), Merck (funding, drug), 3M (drug), Theraclion (device staff support); Funding to the University of Virginia from Polynoma for PI role on the MAVIS Clinical Trial; Funding to the University of Virginia for roles on Scientific Advisory Boards for CureVac. Also Dr. Slingluff receives licensing fee payments through the UVA Licensing and Ventures Group for patents for peptides used in cancer vaccines. The other authors do not have any financial conflicts to disclose relevant to this manuscript.

Funding

Support provided by the US Public Health Services Training Grant T32HL007849 (KL), an internal grant from the UVA Department of Surgery (ISM), the Rebecca Clary Harris Memorial Fellowship from the University of Virginia (KL, NLE), the Harrison grant from the University of Virginia (PK), and a Melanoma Research Alliance Established Investigator Award (VHE). Additional support was received from the University of Virginia Cancer Center Support Grant (NIH P30 CA044579), and NIH/NCI K25CA181638.

Abbreviations

Primary desmoplastic melanoma (PDM), non-desmoplastic metastatic melanoma (NDMM), desmoplastic melanoma (DM), tertiary lymphoid structures (TLS), multiplex immunofluorescence histology (mIFH), immune checkpoint blockade (ICB), tumor infiltrating lymphocytes (TIL), high endothelial venules (HEV), dendritic cells (DC), lymph nodes (LN), regions of interest (ROI), tumor microenvironment (TME)

Data availability statement

All data are available from the authors on reasonable request.

Contributorship

Conception and design: IM, CLS. Development and execution of methodology: IM, PK. Acquisition of data: IM, NLE, SEG. Analysis and interpretation of data (e.g., statistical analysis, computational analysis): NLE, IM and CLS. Writing, review and/or revision of the manuscript: NLE, IM, CLS, VE, KL, AMS, AAG. Administrative, technical, or material support (assisting in experiments): ISM, PK.

References

1. Eroglu Z, Zaretsky JM, Hu-Lieskovan S, et al. High response rate to PD-1 blockade in desmoplastic melanomas. Nature. 2018;553 (7688):347–350. doi:10.1038/nature25187.
2. Ochoa CE, Joseph RW. Desmoplastic melanoma: a brief review and the efficacy of immunotherapy. Expert Rev Anticancer Ther. 2019;19(3):205–207. doi:10.1080/14737140.2019.1574573.
3. Stowman AM, Hickman AW, Mauldin IS, Mahmutovic A, Gru AA, Slingluff CL. Lymphoid aggregates in desmoplastic melanoma have features of tertiary lymphoid structures. Melanoma Res. 2018;28(3):237–245. doi:10.1097/CMR.0000000000000439.
4. Dieu-Nosjean MC, Goc J, Giraldo NA, Sautès-Fridman C, Fridman WH. Tertiary lymphoid structures in cancer and beyond. Trends Immunol. 2014;35(11):571–580. doi:10.1016/j.it.2014.09.006.
5. Rodriguez AB, Peske JD, Woods AN, Leick KM, Mauldin IS, Meneveau MO, Young SJ, Lindsay RS, Melssen MM, Cyranowski S, et al. Immune mechanisms orchestrate tertiary lymphoid structures in tumors via cancer-associated fibroblasts. Cell Rep. 2021;36(3):109422. doi:10.1016/j.celrep.2021.109422.
6. Rangel-Moreno J, Moyron-Quiroz JE, Hartson L, Kusser K, Randall TD. Pulmonary expression of CXC chemokine ligand 13, CC chemokine ligand 19, and CC chemokine ligand 21 is essential for local immunity to influenza. Proc Natl Acad Sci. 2007;104 (25):10577–10582. doi:10.1073/pnas.0700591104.
7. Fleige H, Ravens S, Moschovakis GL, Bölter J, Willenzon S, Sutter G, Häussler S, Kalinke U, Prinz I, Förster R, et al. IL-17–induced CXCL12 recruits B cells and induces follicle formation in BALT in the absence of differentiated FDCs. J Exp Med. 2014;211 (4):643–651. doi:10.1084/jem.20131737.
8. Barone F, Nayar S, Campos J, Cloake T, Withers DR, Toellner K-M, Zhang Y, Fouser L, Fisher B, Bowman S, et al. IL-22 regulates lymphoid chemokine production and assembly of tertiary lymphoid organs. Proc Natl Acad Sci. 2015;112 (35):11024–11029. doi:10.1073/pnas.1503315112.
9. Domblides C, Rochefort J, Riffard C, Panouillot M, Lescaille G, Teillaud J-L, Mateo V, Dieu-Nosjean M-C. Tumor-associated tertiary lymphoid structures: from basic and clinical knowledge to therapeutic manipulation. Front Immunol. 2021;12:698604. doi:10.3389/fimmu.2021.698604.

10. Helmink BA, Reddy SM, Gao J, Zhang S, Basar R, Thakur R, Yizhak K, Sade-Feldman M, Blando J, Han G, et al. B cells and tertiary lymphoid structures promote immunotherapy response. Nature. 2020;577(7791):549–555. doi:10.1038/s41586-019-1922-8.
11. Lynch KT, Young SJ, Meneveau MO, Wages NA, Engelhard VH, Slingluff Jr CL, Mauldin IS. Heterogeneity in tertiary lymphoid structure B-cells correlates with patient survival in metastatic melanoma. J Immunother Cancer. 2021;9(6):e002273. doi:10.1136/jitc-2020-002273.
12. Goc J, Fridman WH, Sautès-Fridman C, Dieu-Nosjean MC. Characteristics of tertiary lymphoid structures in primary cancers. Oncoimmunology. 2013;2(12):e26836. doi:10.4161/onci.26836.
13. Gershenwald JE, Scolyer RA, Hess KR, Sondak VK, Long GV, Ross MI, Lazar AJ, Faries MB, Kirkwood JM, McArthur GA, et al. Melanoma staging: evidence-based changes in the American Joint Committee on Cancer eighth edition cancer staging manual: melanoma Staging: AJCC 8 th Edition. CA Cancer J Clin. 2017;67(6):472–492. doi:10.3322/caac.21409.
14. Schneider CA, Rasband WS, Eliceiri KW. NIH Image to ImageJ: 25 years of image analysis. Nat Methods. 2012;9(7):671–675. doi:10.1038/nmeth.2089.
15. Shain AH, Garrido M, Botton T, Talevich E, Yeh I, Sanborn JZ, Chung J, Wang NJ, Kakavand H, Mann GJ, et al. Exome sequencing of desmoplastic melanoma identifies recurrent NFKBIE promoter mutations and diverse activating mutations in the MAPK pathway. Nat Genet. 2015;47(10):1194–1199. doi:10.1038/ng.3382.
16. Cerami E, Gao J, Dogrusoz U, Gross BE, Sumer SO, Aksoy BA, Jacobsen A, Byrne CJ, Heuer ML, Larsson E, et al. The cBio cancer genomics portal: an open platform for exploring multidimensional cancer genomics data. Cancer Discov. 2012;2(5):401–404. doi:10.1158/2159-8290.CD-12-0095.
17. Gao J, Aksoy BA, Dogrusoz U, Dresdner G, Gross B, Sumer SO, Sun Y, Jacobsen A, Sinha R, Larsson E, et al. Integrative analysis of complex cancer genomics and clinical profiles using the cBioPortal. Sci Signal. 2013;6(269). doi:10.1126/scisignal.2004088
18. Hiraoka N, Ino Y, Yamazaki-Itoh R, Kanai Y, Kosuge T, Shimada K. Intratumoral tertiary lymphoid organ is a favourable prognosticator in patients with pancreatic cancer. Br J Cancer. 2015;112(11):1782–1790. doi:10.1038/bjc.2015.145.
19. Chen C, Gao FH. Th17 cells paradoxical roles in melanoma and potential application in immunotherapy. Front Immunol. 2019;10:187. doi:10.3389/fimmu.2019.00187.
20. Werner F, Wagner C, Simon M, Glatz K, Mertz KD, Läubli H, Griss J, Wagner SN. A standardized analysis of tertiary lymphoid structures in human melanoma: disease progression- and tumor site-associated changes with germinal center alteration. Front Immunol. 2021;12:675146. doi:10.3389/fimmu.2021.675146.
21. Cipponi A, Mercier M, Seremet T, Baurain J-F, Théate I, van den Oord J, Stas M, Boon T, Coulie PG, van Baren N, et al. Neogenesis of lymphoid structures and antibody responses occur in human melanoma metastases. Cancer Res. 2012;72(16):3997–4007. doi:10.1158/0008-5472.CAN-12-1377.
22. Busam KJ, Mujumdar U, Hummer AJ, Nobrega J, Hawkins WG, Coit DG, Brady MS. Cutaneous desmoplastic melanoma: reappraisal of morphologic heterogeneity and prognostic factors. Am J Surg Pathol. 2004;28(11):1518–1525. doi:10.1097/01.pas.0000141391.91677.a4.
23. Cabrita R, Lauss M, Sanna A, Donia M, Skaarup Larsen M, Mitra S, Johansson I, Phung B, Harbst K, Vallon-Christersson J, et al. Tertiary lymphoid structures improve immunotherapy and survival in melanoma. Nature. 2020;577(7791):561–565. doi:10.1038/s41586-019-1914-8.
24. Kendra KL, Moon J, Eroglu Z, Hu-Lieskovan S, Carson WE, Wada DA, Plaza JA, In GK, Ikeguchi A, Hyngstrom JR, et al. Neoadjuvant PD-1 blockade in patients with resectable desmoplastic melanoma (SWOG 1512). J Clin Oncol. 2022;40(16_suppl):9502. doi:10.1200/JCO.2022.40.16_suppl.9502.